Acta Cryst. (1975). A31, 417

Extinction within the Limit of Validity of the Darwin Transfer Equations. III. Non-Spherical Crystals and Anisotropy of Extinction

BY PIERRE J. BECKER

Centre de Mécanique Ondulatoire Appliquée, 23 Rue du Maroc, 75019 Paris, France

AND PHILIP COPPENS

Chemistry Department, State University of New York at Buffalo, Acheson Hall, Buffalo, New York 14214, *U.S.A.*

(*Received* 29 *August* 1974; *accepted* 20 *January* 1975)

Previously derived formalisms for extinction are extended to include crystals of non-spherical shape and anisotropy of mosaic spread and particle size. Expressions derived for extinction in an ellipsoidal crystal are compared with numerical calculations on a polyhedral specimen. A pseudo-spherical approximation for polyhedral crystals is described which is accurate to within 2% of the extinction factor y for crystals whose ratio of maximum and minimum dimensions is less than two. Anisotropy of mosaic spread is introduced in both the Coppens–Hamilton (C.H.) and Thornley–Nelmes (T.N.) descriptions, with both a Lorentzian or a Gaussian distribution function. The formalisms are applied to neutron data sets on $LiTbF_4$ (100°K and 300°K), tetracyanoethylene and $LiOH.H_2O$, and an X-ray data set on α-deutero oxalic acid dihydrate. The distinction between type I and type II crystals is quite clear on the basis of a comparison of R values. Only for LiF, which was studied earlier, was extinction dominated by particle size. In all other cases the best fit corresponds to mosaic-spread-dominated extinction, with a Lorentzian shape of the distribution function. This is especially clear when partial R values summed over the severely extinction-affected reflections are compared. The new formalisms are further supported by the consistency of the final parameters among various refinements in which the most severely extinction-affected reflections are eliminated. Simultaneous refinement on both the particle size and the mosaic spread was only successful in the earlier studied case of SrF_2. The T.N. description of anisotropy leads to lower partial R values, in agreement with physical arguments supporting the validity of this distribution.

Introduction

A general treatment of extinction in X-ray and neutron single-crystal diffractometry has been published recently (Becker & Coppens, 1973, 1974*a* – here referred to as A). This formalism removes several inadequacies of the theory of Zachariasen (1967) and takes the variation of the extinction correction with the scattering and setting angles explicitly into account. As the physical approximations used assume an incoherent manyfold rescattering of the beams inside the crystal, the model is more adequate in its description of the secondary extinction process involving scattering in different mosaic blocks than in its description of the primary extinction process inside a perfect crystal.

A general solution was found to the basic equations of transfer of intensity in the case of a convex shaped crystal. The theory is not adequate when applied to a perfect semi-infinite crystal, but agrees reasonably well with a first-order dynamical calculation for a perfect sphere; it may therefore be considered to give a reasonable description of primary extinction in crystallites of regular shape.

Detailed calculations were first performed for spherical crystals with isotropic extinction, in which case the only angular dependence is on the Bragg angle θ. Analysis of the effect of absorption led to the conclusion that extinction and absorption cannot be treated independently if $\mu R > 0{\cdot}50$.

Both the dimension of perfect crystallites and the mosaic distribution were derived for SrF_2, and the agreement between parameters obtained with the three different wavelengths sets was satisfactory. The particle size of the LiF sample was shown to be physically reasonable (Becker & Coppens, 1974*b* – here referred to as B).

Four general conclusions can be drawn from articles A and B.

(i) the angular dependence of extinction must be properly incorporated in the formalism.

(ii) when extinction is severe, it is dominated by mosaic spread (type I), except for very low scattering angles.

(iii) a choice between extinction dominated by type I or type II is usually possible on the basis of the R values.

(iv) the mosaic angular distribution seems more likely to be Lorentzian than Gaussian.

In the present article, the formalism is applied to non-spherical crystals. Anisotropic extinction, introduced by Coppens & Hamilton (1970) in the Zachariasen approximation, is also introduced. The validity and possible extensions of a 'pseudo-spherical approximation' are discussed. A general modification

of the least-squares routine *LINUS* is applied to four examples (one X-ray and three neutron data sets), which have been selected in order to test the limits of the theory. The notations are those of articles A and B (see Appendix *E* of article A).

I. Generalization of the formalism

The effect of the anisotropy of the crystal shape will be discussed for an ellipsoidal crystal. The conclusions are compared with numerical calculations on a polyhedral crystal to derive an approximate treatment of practical importance.

Transformation of an ellipsoid into a sphere

An ellipsoid (E) may be defined with respect to its principal axes $\mathbf{a}_1, \mathbf{a}_2, \mathbf{a}_3$. If p_i are the components of a vector along $\mathbf{a}_i$, the equation of (E) is:

$$\sum_{i=1}^{3} \left(\frac{p_i}{a_i}\right)^2 = 1 \ . \tag{1}$$

The radii r_0 and r of (E) along the incident and diffracted directions $\mathbf{u}_0$ and $\mathbf{u}$ are given by:

$$r_0^{-2} = \sum_{i=1}^{3} \left(\frac{u_{0i}}{a_i}\right)^2$$

$$r^{-2} = \sum_{i=1}^{3} \left(\frac{u_i}{a_i}\right)^2 . \tag{2}$$

(E) can be transformed into a sphere (S) of radius R by a product of three orthogonal affinity transformations along $\mathbf{a}_i$ and of respective ratios (R/a_i). This procedure has been used previously by Weber (1963) to calculate the absorption correction in an ellipsoid. The coordinates p_i of a point transform to q_i, given by:

$$q_i = p_i \frac{R}{a_i}, \quad i = 1,2,3 . \tag{3}$$

The vectors $\mathbf{u}_0$ and $\mathbf{u}$ transform to new directions with unit vectors $\mathbf{u}_0'$ and $\mathbf{u}'$, whose mutual angle is $2\theta'$. If the transformed path lengths along $\mathbf{u}_0'$ and $\mathbf{u}'$ are defined as S_1 and S_2' [Fig. 1(*b*)], one gets:

$$S_1 = \frac{T_1}{k_1} \quad S_2' = \frac{T_2'}{k_2} \tag{4}$$

with

$$k_1 = \frac{r_0}{R} \quad k_2 = \frac{r}{R} .$$

The angle θ' satisfies the equation:

$$\cos 2\theta' = \sum_{i=1}^{3} u_{0i} u_i \frac{r_0 r}{a_i^2} . \tag{5}$$

In a more general definition of an ellipsoid by a tensor $\mathbf{E}$ with principal values $(1/a_i^2)$, in a space described by a metric G, (1), (2), and (5) become:

$$\mathbf{P}^t\mathbf{E}\mathbf{P} = 1 \tag{1'}$$

$$r_0 = (\mathbf{u}_0^t \mathbf{E} \mathbf{u}_0)^{-1/2}; \quad r = (\mathbf{u}^t \mathbf{E} \mathbf{u})^{-1/2} \tag{2'}$$

$$\cos 2\theta' = r_0 r \mathbf{u}_0^t \mathbf{E} \mathbf{u} . \tag{5'}$$

Diffracting unit cross section for an ellipsoid

It was shown in A that the diffracting unit cross section $\sigma(\varepsilon_1)$ is given, for a convex shaped crystal, by:

$$\sigma(\varepsilon_1) = Q\alpha v^{-1} \int_{\text{crystal}} dv \ \frac{\sin^2(\pi\varepsilon_1\alpha)}{(\pi\varepsilon_1\alpha)^2} \tag{6a}$$

with

$$\alpha = l \sin 2\theta/\lambda , \tag{6b}$$

l being the local thickness of the crystal along the diffracted beam direction.

Using the results of the previous section, it is straightforward to show that $\sigma_E(\varepsilon_1)$ is related to the corresponding value $\sigma_{\text{sphere}}(\varepsilon_1)$ for a sphere by:

$$\sigma_E(\varepsilon_1) = k_2 \sigma_{\text{sphere}}(k_2 \varepsilon_1) . \tag{7}$$

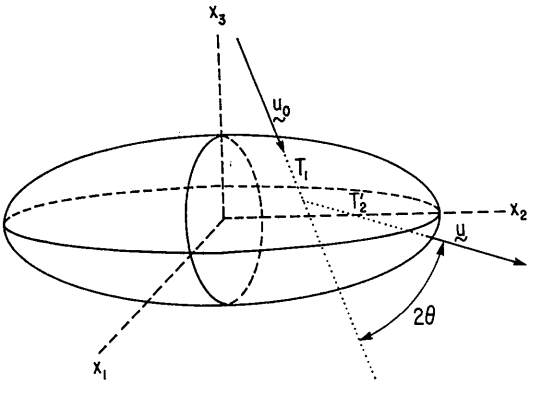

(*a*)

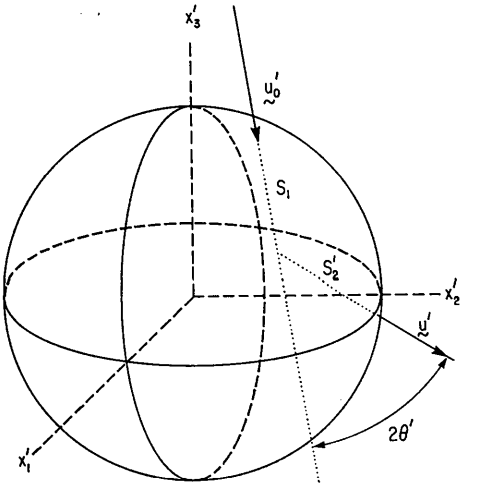

(*b*)

Fig. 1. (*a*) Incident and diffracted beams in an ellipsoidal crystal. (*b*) The affinity transformation of the ellipsoid into a sphere.

Therefore, the equation A-(29) remains valid for an ellipsoid, r becoming the radius along the direction $\mathbf{u}$ [equation (2) or (2′)]. The effective particle size $\bar{\alpha}$ defined in A-(35*b*) is given by:

$$\bar{\alpha}=\tfrac{3}{2}(\mathbf{u}^t\mathbf{E}\mathbf{u})^{-1/2}\sin 2\theta/\lambda\,. \tag{8}$$

For anisotropic primary extinction or anisotropic type II secondary extinction where the average perfect crystallite is approximated by an ellipsoid, (8) will replace its isotropic analog in the expressions for the parameters x_p and x_s. In comparison with the earlier expression by Coppens & Hamilton (1970), $\mathbf{u}$ replaces the normal $\mathbf{N}$ to the incident beam in the diffraction plane and the factor $\sin 2\theta$ is added; these revisions have been discussed in detail in article A.

Anisotropy of the mosaic spread distribution

Coppens & Hamilton (1970) have introduced anisotropy in the angular mosaic distribution W (and the mosaic spread parameter η):

$$W(\varepsilon_1,\mathbf{D})=\det(Z)^{1/2}2^{3/2}\exp(-2\pi\varepsilon^2\mathbf{D}^t\mathbf{Z}\mathbf{D})$$

$$\eta(\mathbf{D})=\frac{1}{2\pi^{1/2}g(D)}=2^{-1}\pi^{-1/2}(\mathbf{D}^t\mathbf{Z}\mathbf{D})^{-1/2}\,. \tag{9}$$

The quantity $g(\mathbf{D})$ is the generalization of the isotropic parameter g: $\mathbf{D}$ is the unit vector normal to the diffraction plane defined by $\mathbf{u}_0$ and $\mathbf{u}$. The representation surfaces of the mosaic spread are ellipsoids whose radii in a given direction are proportional to the mosaic spread η perpendicular to that direction. Generalizing a discussion by Nelmes (1969) of the indicatrix ellipsoids for thermal motion, Thornley & Nelmes (1974) have proposed the following alternative form for the mosaic angular distribution:

$$W'(\varepsilon_1,\mathbf{D})=(\mathbf{D}^t\mathbf{Y}\mathbf{D})^{-1/2}2^{1/2}\exp\left(\frac{-2\pi\varepsilon_1^2}{\mathbf{D}^t\mathbf{Y}\mathbf{D}}\right)$$

$$\eta'(\mathbf{D})=\frac{1}{2\pi^{1/2}g'(\mathbf{D})}=2^{-1}\pi^{-1/2}(\mathbf{D}^t\mathbf{Y}\mathbf{D})^{1/2}\,. \tag{10}$$

With the distribution given by (10), the representation surfaces are ellipsoids with radii inversely proportional to the mosaic spread η' about the direction under study.

Thornley & Nelmes (1974) discussed the variation of extinction for a given reflection of a boracite, on rotation of the crystal around the diffraction vector; they found (10) to fit these experimental data better than (9).

Analogous expressions can be derived for a Lorentzian distribution; they are:

$$W(\varepsilon_1,\mathbf{D})=\frac{2(\mathbf{D}^t\mathbf{Z}\mathbf{D})^{1/2}}{1+4\pi^2\varepsilon_1^2\mathbf{D}^t\mathbf{Z}\mathbf{D}}$$

$$\eta(\mathbf{D})=\frac{(2\pi)^{-1}}{g(\mathbf{D})}=(2\pi)^{-1}(\mathbf{D}^t\mathbf{Z}\mathbf{D})^{-1/2} \tag{11}$$

$$W'(\varepsilon_1,\mathbf{D})=\frac{2(\mathbf{D}^t\mathbf{Y}\mathbf{D})^{-1/2}}{1+\dfrac{4\pi^2\varepsilon_1^2}{\mathbf{D}^t\mathbf{Y}\mathbf{D}}}$$

$$\eta'(\mathbf{D})=\frac{(2\pi)^{-1}}{g'(\mathbf{D})}=(2\pi)^{-1}(\mathbf{D}^t\mathbf{Y}\mathbf{D})^{1/2}\,. \tag{12}$$

The effect of anisotropy of the crystal shape on the extinction parameter

Applying the affinity transformation defined by (3), one can relate $\varphi_E(\bar{\sigma},\theta)$ for the ellipsoid (E) to the corresponding function φ_{sphere} for a sphere: [equations A-(17) and A-(21)]

$$\varphi_E(\bar{\sigma},\theta)=v_{\text{sphere}}^{-1}\int_{\text{sphere}}\mathrm{d}v_{\text{sphere}}\times\exp-\bar{\sigma}(k_1S_1+k_2S_2')\mathscr{J}_0(2i\bar{\sigma}\sqrt{k_1k_2}\sqrt{S_1S_2'}). \tag{13}$$

When the scattering angle θ is small, one can write:

$$k_1\sim k_2\sim k$$

and (13) leads to:

$$\varphi_E(\bar{\sigma},\theta)=\varphi_{\text{sphere}}(k\bar{\sigma},\theta')\,. \tag{14}$$

Since the actual value of the mean path length $\bar{T}$ through the crystal is $k\bar{T}_{\text{sphere}}$ in that case, if one defines x_s as in A (35*a*) and B by:

$$x_s=\tfrac{2}{3}Q\alpha_{G,L}\bar{T} \tag{15}$$

one gets for the secondary extinction correction:

$$y_s=y_s^{\text{sphere}}(x_s,\ \theta')\,. \tag{16}$$

(16) shows that at small Bragg angles the only effect of the anisotropy of the crystal shape is a replacement of θ by θ', provided x_s is defined by (15).

In the general case, let:

$$k=(k_1k_2)^{1/2}=(r_0r)^{1/2}R^{-1}$$

$$\varrho=\left(\frac{k_1}{k_2}\right)^{1/2}=\left(\frac{r_0}{r}\right)^{1/2}\,. \tag{17}$$

ϱ^2 represents the anisotropy coefficient of the crystal for a given reflection. (13) transforms to:

$$\varphi_E(\bar{\sigma},\theta)=v_{\text{sphere}}^{-1}\int_{\text{sphere}}\mathrm{d}v_{\text{sphere}}\exp-k\bar{\sigma}(\varrho S_1+\varrho^{-1}S_2')\times\mathscr{J}_0(2ik\bar{\sigma}\sqrt{S_1S_2'})\,. \tag{18}$$

x_s is given by

$$x_s=\tfrac{2}{3}Q\alpha_{G,L}\bar{T}_{\text{sphere}}\frac{k}{2}(\varrho+\varrho^{-1})\,. \tag{19}$$

Therefore, when using this expression for x_s, the only new anisotropic effect is associated with ϱ. Using the same numerical procedure as described in article A, computations of the extinction correction as a function of x_s, were performed for various values of θ' and ϱ, for a Lorentzian and a Gaussian angular mosaic distribution (Becker, 1973). The results, which are similar for the two distributions, are shown in Fig. 2

for a Lorentzian distribution. Since the extinction effect is usually found to be small for large angles, one may assume that the explicit variation of y_s with ϱ is negligible when ϱ is smaller than about 1·4, *i.e.* when the anisotropy is smaller than 2. From the calculations for large values of ϱ, it is possible to modify the expression for the parameters $A(\theta')$ and $B(\theta')$ in the function $y_s(x_s,\theta')$ [expression A-(37) and B-(4)], including an explicit variation with ϱ.

A real crystal is generally polyhedral and poorly described by an ellipsoid. It would therefore be convenient to use (16) if the anisotropy of the crystal is less than 2, provided the value of the mean path length, $\bar{T}$, is computed for each reflection from the actual crystal shape. The only effect to consider is that associated with the transformation $\theta \rightarrow \theta'$. We shall examine this point for a crystal of tetracyanoethylene (TCNE) which has been used in a neutron diffraction experiment (Becker, Coppens & Ross, 1973) and shows severe and anisotropic extinction. The crystal structure is cubic and the sample is a parallelepiped of dimensions $2{\cdot}1 \times 2{\cdot}6 \times 3{\cdot}2$ mm parallel to **a**, **b**, **c** respectively. For various sets of reflections of given Bragg angles, the extinction correction was numerically calculated as a function of x_s. Some of the results are shown in Fig. 3 and are compared with the pseudo-spherical approximation in which θ' is taken to be equal to θ. For the low-order reflections [Fig. 3(*a*)], that are the more severely affected by extinction, the spherical approximation (with actual values of $\bar{T}$) is a satisfactory average of the curves differing with the setting of the crystal, even for large values of x_s. When the Bragg angle increases, the range of validity of the pseudo-spherical approximation becomes smaller, but at the same time, because the reflections tend to be weaker, y_s becomes closer to one. The agreement therefore remains good for the actual range of x_s. It follows that *a pseudo-spherical treatment (with $\bar{T}$ for a polyhedral crystal, but $\theta'=\theta$) is a reasonable approximation (precision better than 2% on y_s) for any crystal whose anisotropy is smaller than two.*

Modifications of the refinement program

A new version *LINEX* 74 of the least-squares routine *LINUS* has been written and is available on request. Various options for the refinement of extinction are included. The calculation of the derivatives follows expressions given earlier.

For example

$$\frac{\partial F^2}{\partial Z_{kl}} = \frac{\partial F^2}{\partial g} \cdot \frac{\partial g}{\partial Z_{kl}}$$

where $\partial F^2/\partial g$ can be found in Table 6 of article B and the expressions for $\partial g/\partial Z_{kl}$ are as given in Table 1 of Coppens & Hamilton (1970). One may refine on secondary extinction of type I or type II, or use a more general formalism. The approximation A-(24):

$$y \sim y_s(x_s) \cdot y_p(x_p)$$

has been replaced by a more realistic one:

$$y \sim y_p(x_p) \cdot y_s[y_p(x_p) \cdot x_s] . \qquad (20)$$

(20) follows from the fact that the actual diffracting unit cross section of the mosaic is $y_p\bar{\sigma}$ instead of $\bar{\sigma}$ (Hamilton, 1957).

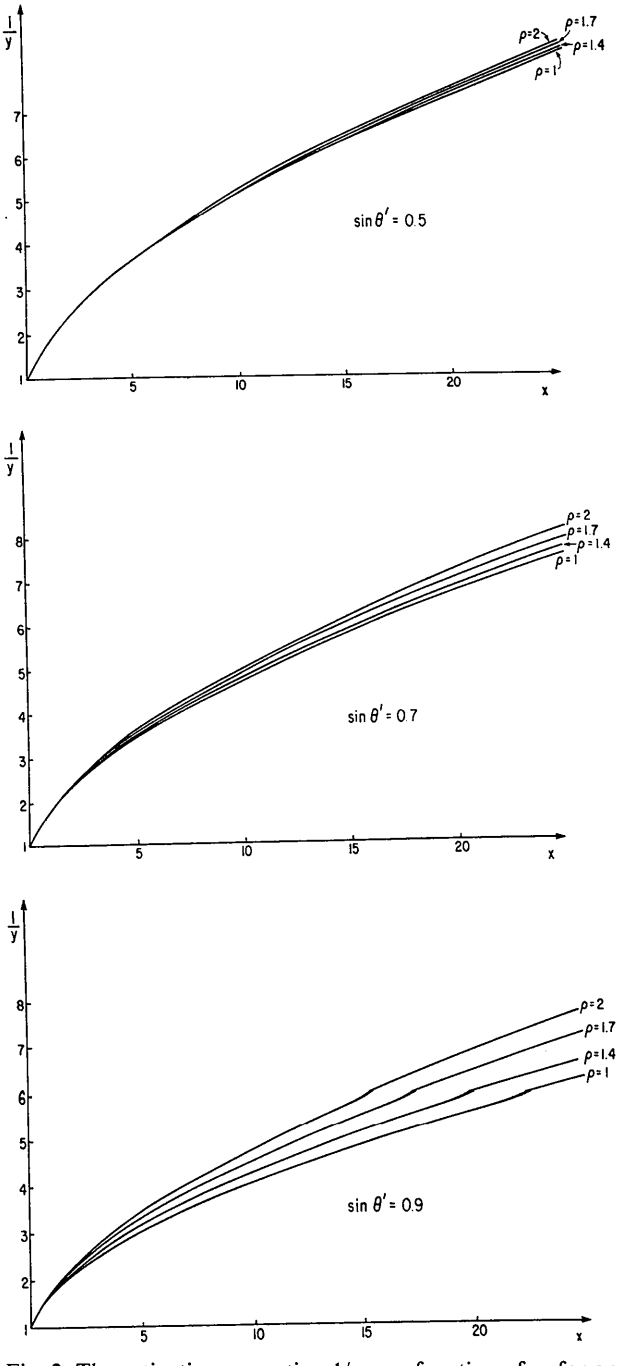

Fig. 2. The extinction correction $1/y$ as a function of x_s for an ellipsoidal crystal at various values of θ and ϱ (Lorentzian distribution).

Extinction may be refined isotropically or anisotropically. For anisotropic type I extinction, the two different definitions of the mosaic anisotropy with either a Gaussian or a Lorentzian distribution [(9)–(10) or (11)–(12)] may be selected, leading to a tensor **Z** or **Y**. In the general case, (intermediate between type I and type II) it would be necessary to refine on two tensors (**E** and either **Z** or **Y**). But, as discussed in A and B, the general expression (20) is only relevant for severe extinction and very small Bragg angles; when applying (20) the particles were constrained to be spherical so that seven rather than twelve parameters had to be determined.

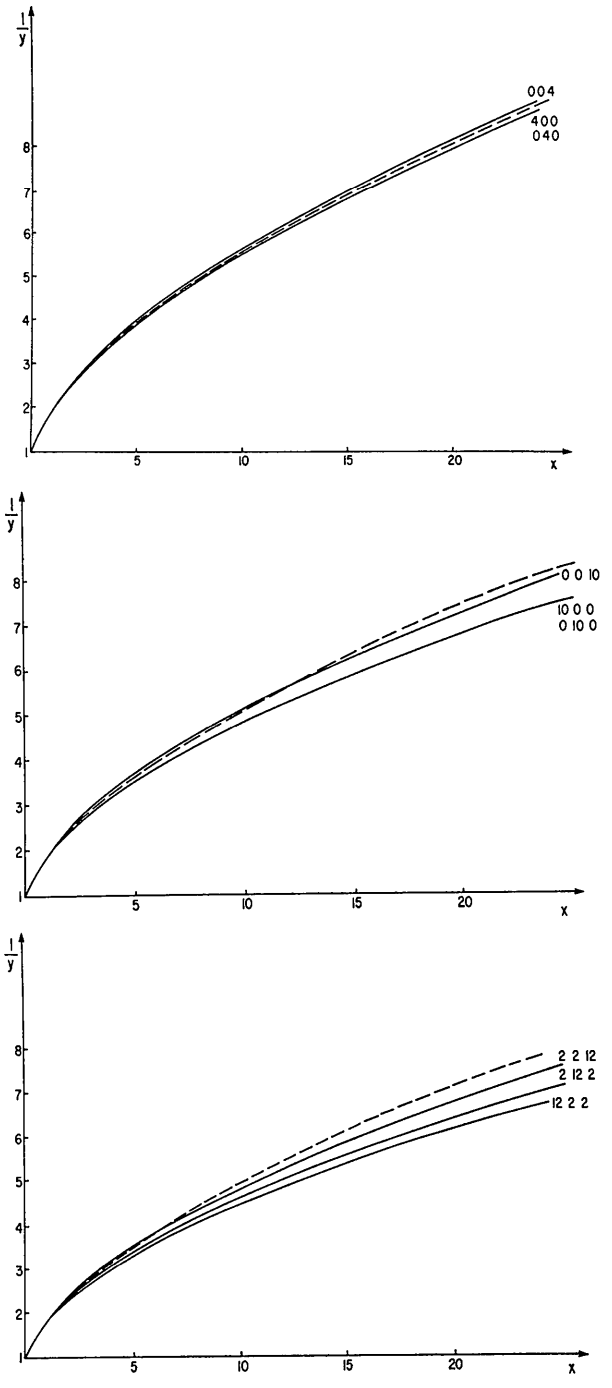

Fig. 3. Numerical results for a number of reflections for a box-shaped TCNE crystal described in the text (full lines), and values obtained in the pseudo-spherical approximation (broken line). The actual values of sin θ and y are as follows: 004, 040 and 400; sin θ=0·208, y=0·13, 0·14 and 0·12 respectively. 10,0,0, 0,10,0 and 0,0,10; sin θ=0·521, y=0·37, 0·44 and 0·39 respectively. 2,2,12, 12,2,2 and 2,12,2; sin θ=0·642, y=0·47, 0·48 and 0·51 respectively.

II. Experimental results

(*a*) $LiTbF_4$ (*neutron data*)

Neutron data, on a large sphere of $LiTbF_4$ were provided by Dr F. K. Larsen of Aarhus University (Als-Nielsen, Holmes, Larsen & Guggenheim, 1974); crystallographic information is summarized in Table 1. Symmetry-equivalent reflections were averaged and extinction was only refined isotropically. In Table 2, R values for various extinction options are compared with a refinement based on the Zachariasen (1967) expressions; the crystals are of type I, with little difference between the agreement for the different distributions. Extinction is moderately severe (the lowest y is equal to 0·37). Atomic parameters not reproduced here are insensitive to the type of refinement. The mosaic spread is very large (26–39′ of arc) and the crystal may be considered as ideally imperfect; it would be of no value to refine on the particle size, (the equivalent particle size being $\sim 10^{-6}$ cm, based on type II extinction; the actual particle dimensions are much larger but small enough for primary extinction to be negligible). In this case, extinction is mainly a result of the large size of the crystal.

Table 1. *Crystallographic information on* $LiTbF_4$

	Space group	$I4_1/a$
Low temperature (L.T.) (100K)	a=5·1805 Å	c=10·873 Å
Room temperature (R.T.)	a=5·1919 Å	c=10·875 Å
	Z=4	

Radius of the spherical crystal	3·5 mm
Wavelength	1·070 Å
Number of observations	196 (L.T.)
	305 (R.T.)

Distribution of y values

	Number of reflections	
Range of y	L.T.	R.T.
0·37 → 0·60	21	13
0·60 → 0·70	26	14
0·70 → 0·80	44	26
0·80 → 0·90	52	75
0·90 → 1	53	177

Since the R value is summed over the complete data set, it is not very sensitive to the fit of the strong, extinction-affected reflections. One may consider partial R values based on reflections in a given range of y, which will be strongly dependent on the extinction

Table 2. *R values for* $LiTbF_4$

	Zach-aria-sen	Type I Gaus-sian	Type I Lorent-zian	Type II
Low temperature				
$R(F^2)$	0·058	0·056	0·056	0·085
$R_w(F^2)$	0·067	0·069	0·066	0·095
PR (F^2)* $(y<0·60)$	0·066	0·074	0·063	
η	26 (1′)	39 (1′)	39 (1′)	
Room temperature				
$R(F^2)$	0·052	0·048	0·049	
$R_w(F^2)$	0·073	0·075	0·072	
PR (F^2)* $(y<0·60)$	0·080	0·073	0·070	
η	28 (1′)	35 (1′)	35 (1′)	

* Here and in the following tables the letters PR indicate partial *R* values.

model when reflections with y larger than about 0·60 are excluded. Such partial *R* values, included in Table 2 indicate that the mosaic distribution is Lorentzian rather Gaussian.

(b) α-Deutero oxalic acid dihydrate (α-DOX) (X-ray data)

This X-ray data set ($\lambda=1·5405$ Å) has been analyzed by Delaplane & Ibers (1969) and Coppens & Hamilton (1970). The crystallographic information is given in Table 3. Extinction is strongly anisotropic, but only severe for few reflections: there are 18 reflections with $y<0·80$ and 32 with $y<0·90$. Coppens & Hamilton (1970) could only refine one type II extinction, and found the temperature parameters to be significantly affected.

Table 3. *Crystallographic information for α-DOX*

Space group $P2_1/n$	
$a=6·150$ (1) Å	$b=3·617$ (1) Å
$c=12·102$ (1) Å	$\beta=106°38$ (1′)
$Z=2$	
Number of observations	546
Temperature	295 K
Lowest y	0·39
Needle-shaped crystal of diameter:	0·22 mm
length:	0·45 mm

We have applied various options to the data set, including all observations in the refinement and assuming isotropic thermal parameters for the deuterium atoms. The refinements were based on *F*. Some *R* values are given in Table 4; it is possible to select type I extinction with a Lorentzian mosaic spread, but a discrimination between the Thornley–Nelmes (T.N.) and the Coppens–Hamilton (C.H.) descriptions is not possible on the basis of full *R* values. However, partial *R* values also given in Table 4 show a pronounced improvement with the new formalism, and indicate a preference for the Thornley–Nelmes description of the mosaic spread. The extinction parameters for the type I Lorentzian refinement are given in Table 5; the atomic parameters do not differ significantly from those previously published.

Table 4. *R values for α-DOX*

	Zacha-riasen Type II	Type I Gaussian T.N. & C.H.	Type I Lorent-zian	Type II
$R(F)$	0·024	0·027	0·022	0·025
$R_w(F)$	0·025	0·028	0·022	0·026
PR (F) $y<0·80$	0·026		0·011 (C.H.) 0·009 (T.N.)	0·018
PR (F) $y<0·90$	0·022		0·012 (C.H.) 0·010 (T.N.)	0·020

Table 5. *Extinction parameters for α-DOX – Lorentzian, type I*

(Thornley–Nelmes) × 10^8		Principal axes and directions	
Y,Z			
11	12·2 (0·7)	η_1	6″ (0,1,0)
22	3·5 (0·2)	η_2	8″ (0·60,0,1·0)
33	8·7 (1)	η_3	15″ (0·85,0,−0·34)
12	0 (0·4)		$(\mathbf{a},\eta_2)=70°$
23	−5·5 (1)		$(\eta_3,\mathbf{a})=20°$
31	0 (0·4)		

(c) Tetracyanoethylene (TCNE) (neutron data)

The neutron diffraction experiment has been discussed previously (Becker, Coppens & Ross, 1973). The results were combined with the X-ray data to yield the valence-electron distribution. Crystallographic information is summarized in Table 6. Extinction is severe. A series of refinements (based on F^2), show that the best fit corresponds to a type I crystal with Lorentzian distribution (Table 7). A simultaneous refinement on both the particle size and the mosaic spread was unsuccessful as *R* values increase significantly. The particle size increased to about 40 μm, which is too large for the model to remain valid when applied to primary extinction effects.

Table 6. *Crystallographic information for TCNE*

Space group $Im3$		
$a=9·736$ (6) Å		
$Z=6$		
Point-group symmetry of the molecules D_{2h}		
$\lambda=1·014$ Å		
Number of observations		503
Number of reflections with	$y<0·2$	12
	$y<0·3$	49
	$y<0·5$	75
Smallest $y=0·09$		

Box-shaped crystal with dimensions 2·1 × 2·6 × 3·2 mm parallel to **a**, **b** and **c**

Partial *R* values (Table 7) show again an improvement with the revised model. There seems to be little preference for either of the two descriptions of the anisotropy of mosaic spread.

Table 7. *R values for TCNE*

	Type I Zachariasen	Type I Gaussian	Type I Lorentzian	Type II	General Type I Lorentzian+Type II +primary extinction
$R(F^2)$	0·055	0·089	0·052	0·094	0·069
$R_w(F^2)$	0·072	0·105	0·068	0·118	0·084
PR $(F^2)y<0·2$	0·13		0·085 (C.H.) 0·085 (T.N.)		
PR $(F^2)y<0·3$	0·10		0·080 (C.H.) 0·078 (T.N.)		

In order to analyze the effect of correlation between thermal parameters and extinction, some refinements were done excluding the reflections with $y<0·2$ or $y<0·3$. Using the Zachariasen formalism, the variation of the temperature parameters as a function of cut-off is small, but systematic, and can reach two standard deviations. On the other hand, with the new expressions, the variation is negligible. In Table 8, the results of the refinements for the Zachariasen correction and for type I Lorentzian extinction are given; the thermal parameters are systematically larger using the revised formalism. Therefore, there is a small reduction of the difference with X-ray thermal parameters (Table 8). It has been pointed out that the deformation density is high compared with other studies and theoretical calculations (Becker, Coppens & Ross, 1973; Coppens, 1974); the systematic bias in the temperature parameters revealed here partly corrects this discrepancy, as it leads to a reduction of almost 0·1 e $Å^{-3}$ in the peak heights (Becker & Coppens, unpublished results).

Table 8. *Results for the thermal parameters for TCNE*

		Zachariasen Type I	Lorentzian Type I	X-ray
N	U_{11}	0·0451 (4)	0·0461 (3)	0·0507 (7)
	U_{22}	0·0453 (4)	0·0462 (3)	0·0479 (6)
	U_{33}	0·0300 (4)	0·0309 (3)	0·0403 (6)
	U_{13}	−0·0139 (2)	−0·0138 (2)	−0·0094 (4)
C(1)	U_{11}	0·0311 (4)	0·0317 (4)	0·0346 (6)
	U_{22}	0·0306 (4)	0·0315 (4)	0·0319 (5)
	U_{33}	0·0239 (4)	0·0249 (4)	0·0299 (6)
	U_{13}	−0·0039 (2)	−0·0039 (2)	−0·0009 (4)
C(2)	U_{11}	0·0277 (5)	0·0288 (4)	0·0355 (8)
	U_{22}	0·0254 (5)	0·0261 (4)	0·0253 (6)
	U_{33}	0·0195 (5)	0·0207 (4)	0·0257 (7)

The T.N. extinction parameters are given in Table 9. The standard deviations for the extinction parameters are reduced by a factor of two compared with the correction of Zachariasen.

(*d*) $LiOH.H_2O$ (*neutron data*)

The data set and the results of earlier refinements have been provided by Dr W. R. Busing. Crystallographic information is summarized in Table 10. Extinction is extremely severe. We have made various refinements, based on F^2. With the Zachariasen correction, it is impossible to refine on the scale factor, because of its correlation with extinction. A refinement assuming extinction to be of type II does not converge. The best fit corresponds to a type I Lorentzian extinction. *R* values are very sensitive to the type of correction. Because of the large size of the perfect blocks, it is not possible to refine on the particle size; the theory incorrectly describes primary extinction in this case.

Table 9. *Extinction parameter for TCNE–Lorentzian, type* I

Y,Z	T.N. (×10⁸)
11	0·0096 (6)
22	0·0202 (20)
33	0·0140 (14)
12	−0·0040 (10)
13	0·0010 (80)
23	0·0000 (160)
Principal axes and directions	
η_1	0·37″ (0,0,1)
η_2	0·3″ (0·27,0·96,0)
η_3	0·46″ (0·96,−0·27,0)
$(\mathbf{a},\eta_2)=60°$	$(\mathbf{a},\eta_2)=75°$
$(\eta_3,\mathbf{a})=30°$	$(\eta_3,\mathbf{a})=15°$

Table 10. *Crystallographic information for* $LiOH.H_2O$

Space group	*C*2/*m*	
$a=7·4153$ (1) Å	$b=8·3054$ (1) Å	
$c=3·1950$ (1) Å	$\beta=110°6'$ (1′)	
$Z=4$		
Wavelength		1·2459 Å
Anisotropy of the polyhedral crystal		<2
Number of observations		609
Number of reflections with	$y<0·1$	60
	$y<0·2$	180
	$y<0·5$	450
Smallest $y=0·04$		

The results of the best refinements are given in Tables 11 and 12 together with the results from an X-ray experiment of average quality described by Alcock (1971). Partial *R* values (Table 11) again confirm a preference for T.N. type mosaic spread.

It is clear from Table 12 that Zachariasen refinement leads to thermal parameters which are quite different from the Lorentzian type I new correction, the present theory being in reasonable agreement with the X-ray results.

In order to test the correlation between temperature parameters and extinction, we have made some refinements where reflections with $y<0·1$ or $y<0·2$ were excluded. With the Zachariasen correction, some

Table 11. *R values for* $LiOH.H_2O$

	Zachariasen Type I	Lorentzian Type I	
		C.H.	T.N.
$R(F^2)$	0·078	0·080	0·076
$R_w(F^2)$	0·087	0·088	0·084
PR (F^2) $y<0·1$	0·068	0·062	0·058
PR (F^2) $y<0·2$	0·072	0·065	0·063

Table 12. *Parameters from refinements of* $LiOH.H_2O$

		Zachariasen Type I	Lorentzian Type I	X-ray
(*a*)				
Li	y	0·3479 (5)	0·3475 (5)	0·3474 (10)
	U_{11}	0·0137 (18)	0·0223 (17)	0·0202 (25)
	U_{22}	0·0091 (19)	0·0194 (18)	0·0160 (30)
	U_{33}	0·0179 (21)	0·0246 (20)	0·0248 (40)
	U_{13}	0·0031 (17)	0·0050 (17)	0·0059 (30)
(*b*)				
O(1)	x	0·2858 (2)	0·2859 (2)	0·2857 (5)
	z	0·3957 (5)	0·3950 (5)	0·3952 (12)
	U_{11}	0·0076 (7)	0·0157 (6)	0·0169 (12)
	U_{22}	0·0101 (8)	0·0199 (7)	0·0182 (15)
	U_{33}	0·0177 (10)	0·0257 (8)	0·0219 (18)
	U_{13}	0·0000 (7)	0·0034 (6)	0·0042 (15)
(*c*)				
O(2)	y	0·2069 (2)	0·2066 (1)	0·2066 (4)
	U_{11}	0·0148 (8)	0·0234 (7)	0·0263 (17)
	U_{22}	0·0082 (7)	0·0179 (7)	0·0206 (20)
	U_{33}	0·0143 (9)	0·0226 (7)	0·0181 (20)
	U_{13}	0·0019 (7)	0·0054 (7)	0·0073 (15)
(*d*)				
H(1)	x	0·2654 (4)	0·2653 (5)	
	z	0·6730 (10)	0·6736 (10)	
	U_{11}	0·0292 (15)	0·0398 (14)	
	U_{22}	0·0356 (17)	0·0452 (17)	
	U_{33}	0·0296 (18)	0·0374 (17)	
	U_{13}	0·0112 (14)	0·0163 (13)	
H(2)	x	0·1114 (3)	0·1117 (3)	
	y	0·1328 (3)	0·1327 (2)	
	z	0·1388 (7)	0·1383 (5)	
	U_{11}	0·0229 (10)	0·0310 (9)	
	U_{22}	0·0215 (10)	0·0313 (10)	
	U_{33}	0·0288 (11)	0·0379 (10)	
	U_{12}	0·0019 (7)	0·0017 (7)	
	U_{13}	0·0065 (10)	0·0105 (9)	
	U_{23}	−0·0009 (8)	−0·0008 (8)	
Z, Y, X $10^{\mp 8}$			(C.H.)	(T.N.)
11		1200 (80)	163 (30)	0·0053 (10)
22		660 (87)	107 (20)	0·0077 (15)
33		1710 (70)	220 (40)	0·0033 (7)
12		63 (47)	12 (7)	−0·0009 (3)
13		−960 (62)	−107 (22)	0·0000 (2)
23		−106 (44)	−15 (7)	0·0000 (2)

(*a*) $x=0$, $z=\frac{1}{2}$, $U_{12}=U_{23}=0$; (*b*) $y=0$, $U_{12}=U_{23}=0$; (*c*) $x=0$, $z=0$, $U_{12}=U_{23}=0$; (*d*) $y=0$, $U_{12}=U_{23}=0$.

temperature parameters varied by five standard deviations, showing an appreciable bias, while the present treatment is supported by such variations being limited to less than one standard deviation.

Again, the new theory leads to higher values of the thermal parameters.

The approximate principal values and directions of the mosaic spread are given in Table 13.

Table 13. *Mosaic spread, principal axes and directions from Lorentzian type* I *refinement*

	T.N.
η_1	0·32″ (0,1,0)
η_2	0·25″ (1,0,0)
η_3	0·18″ (0·36,0,1·1)
$(\mathbf{a},\eta_2)$	0
$(\mathbf{a},\eta_3)$	90°

III. Discussion

For large data sets R values obtained with the revised formalisms are not very different from those obtained with the Zachariasen correction. However, partial R values limited to intense extinction-affected reflections are much more sensitive to the nature of the extinction formalism, and indicate a preference for the revised model. The standard deviations of the extinction parameters are also reduced significantly.

The distinction between type I and type II extinction is quite pronounced because of the $\sin 2\theta$ dependence of x_s for type II crystals. Only in the case of LiF was extinction dominated by particle size. In all other cases the best fit corresponds to mosaic-spread-dominated extinction, with a Lorentzian shape of the distribution function. It implies that some crystallites are quite misoriented, as the Lorentzian distribution has rather broad tails in comparison with a Gaussian function.

The consistency of the refined parameters from data sets at different wavelengths (for SrF_2) and from refinements eliminating reflections with $y<0·1$, $y<0·2$ and $y<0·3$ (TCNE and LiOH) support application of the new formalisms. Only in the case of SrF_2 was refinement on both the particle size and the mosaic spread successful. In other cases, the particle size is large and has little influence on the secondary extinction, while primary extinction is improperly described in these cases. Fortunately, this affects only few reflections.

The pseudo-spherical approximation, applied to polyhedral crystals, has been shown to be accurate within about 2% if the ratio of the extreme dimensions of the crystal does not exceed a factor of two. For more severe anisotropy and very severe strong extinction it may be necessary to complement the pseudo-spherical refinement with an additional numerical evaluation of y using equation B-(2).

The two descriptions of anisotropic mosaicity

The Thornley & Nelmes description of mosaic anisotropy takes into account the component of the misorientation for all the mosaic blocks which corresponds to a rotation around the vector **D** normal to the diffraction plane. The earlier description (C.H.) takes into account only the distribution in the plane perpendicular to **D** and thereby neglects any effect of a

misorientation in other directions. Especially when the beam is finely collimated such a misorientation will affect the domain distribution $N(\varepsilon_1)$ and its neglect is therefore not justifiable.

It is satisfying that, in cases where a distinction can be made, partial R values favor the T.N. model, in agreement also with experimental measurements of the pronounced variation of the diffracted intensity of a boracite on rotation around the diffraction vector (Thornley & Nelmes, 1974).

Finally, it may be pointed out that though the physical formulation of extinction requires further study, the present theory extends the domain of applicability of an extinction refinement. This is of special importance in neutron diffraction studies, where extinction is often severe. In further development of formalisms it may be necessary to modify or abandon the mosaic model, and to allow for the partial coherence of the multiple diffraction process.

The authors would like to thank Drs F. K. Larsen and W. R. Busing for making the neutron data on $LiTbF_4$ and $LiOH.H_2O$ available prior to publication and Mrs L. Marshall for assistance with the calculations. They are indebted to a referee for many helpful comments. Support of this work by the National Science Foundation is gratefully acknowledged.

References

ALCOCK, N. W. (1971). *Acta Cryst.* B**27**, 1682–1683.
ALS-NIELSEN, J., HOLMES, L. M., LARSEN, F. K. & GUGGENHEIM, H. J. (1975). *Phys. Rev.* B. In the press.
BECKER, P. J. (1973). These d'Etat. Paris.
BECKER, P. J. & COPPENS, P. (1973), 1st European Crystallography Conference, Bordeaux, France.
BECKER, P. J. & COPPENS, P. (1974*a*). *Acta Cryst.* A**30**, 129–147.
BECKER, P. J. & COPPENS, P. (1974*b*). *Acta Cryst.* A**30**, 148–153.
BECKER, P. J., COPPENS, P. & ROSS, F. K. (1973). *J. Amer. Chem. Soc.* **95**, 7604–7609.
COPPENS, P. (1974). *Acta Cryst.* B**30**, 255–261.
COPPENS, P. & HAMILTON, W. C. (1970). *Acta Cryst.* A**26**, 71–83.
DELAPLANE, R. G. & IBERS, J. A. (1969). *Acta Cryst.* A**25**, 2423–2437.
HAMILTON, W. C. (1957). *Acta Cryst.* **10**, 629–634.
NELMES, R. J. (1969). *Acta Cryst.* A**25**, 523–526.
THORNLEY, F. R. & NELMES, R. J. (1974). *Acta Cryst.* A**30**, 748–757.
WEBER, K. (1963). *Acta Cryst.* **16**, 535–542.
ZACHARIASEN, W. H. (1967). *Acta Cryst.* **23**, 558–564.

Acta Cryst. (1975). A**31**, 425

Structure of X-ray Wave Packets in Perfect and Highly Distorted Crystals

BY F. BALIBAR & C. MALGRANGE

Laboratoire de Minéralogie-Cristallographie associé au C.N.R.S., Université Paris VI, *Tour* 16, 4 *place Jussieu*, 75230 *Paris Cedex* 05, *France*

(*Received* 6 *January* 1975; *accepted* 31 *January* 1975)

It is shown that, in order to treat the problem of the propagation of an X-ray wave in a distorted crystal, the plane-wave assumption, which is one of the fundamental ingredients in the usual dynamical theory, should be removed. Both the incident and the crystal waves should be built as *wave packets*, *i.e.* continuous distributions of **K** vectors, characterized by their extensions in both reciprocal and direct spaces. The characteristic structure of the crystal wave packet for a perfect crystal, and the changes undergone by this structure as a result of the crystal distortions, are examined; the criterion for the validity of geometrical optics is thus reformulated.

I. Introduction

The dynamical theory of X-ray diffraction is generally considered to be concerned with the problem of propagation of an electromagnetic wave of given frequency falling in the X-ray region in a medium made up of a more-or-less perfect three-dimensional array of atoms. As a matter of fact, the papers which originated this kind of studies (Ewald, 1916; Darwin, 1914; von Laue, 1931) were only concerned with a very special kind of waves (*i.e.* plane waves) incident on a perfect crystal (*i.e.* a medium without any disturbance in the three-dimensional ordering of atoms). The wave inside the crystal then appears as a superposition of *four plane waves*, the characteristics of which can be fully determined from the boundary conditions at the entrance surface. It was soon realized that in order to deal with real cases one has to extend this ideal treatment (which we shall call the Ewald–Laue theory) to that of a non-plane wave travelling in a non-perfect crystal. This has usually been performed by mere adaptation of the ideal plane-wave solution: the characteristic parameters of the plane-wave solution (*e.g.* the departure from exact Bragg angle) were considered to be space varying and one calculated the change of this 'variable constant' necessary to match the real propagation conditions. Kato's (1963, 1964*a*, *b*), Penning's (1961) and Penning & Polder's (1966) treatments can be considered as typical examples of such a way of dealing with the real problem. For ten